Hindawi
International Journal of Antennas and Propagation
Volume 2023, Article ID 6065300, 9 pages
https://doi.org/10.1155/2023/6065300

Research Article

Polarization Stable Triband Thin Square-Shaped Metamaterial Absorber

M. L. S. N. S. Lakshmi,[1] S. Prasad Jones Christydass,[1] S. Kannadhasan,[2] K. Anguraj,[3] and Jyotir Moy Chatterjee[4]

[1]*Department of ECE, QIS College of Engineering & Technology, Ongole, Andhra Pradesh, India*
[2]*Department of ECE, Study World College of Engineering, Coimbatore, Tamilnadu, India*
[3]*Department of ECE, Sona College of Technology, Salem, Tamilnadu, India*
[4]*Scientific Research Group of Egypt (SRGE), Lord Buddha Education Foundation, Kathmandu, Nepal*

Correspondence should be addressed to Jyotir Moy Chatterjee; jyotirchatterjee@gmail.com

Received 23 September 2022; Revised 13 December 2022; Accepted 22 December 2022; Published 14 January 2023

Academic Editor: Giorgio Montisci

An efficient triband metamaterial absorber is presented for X- and K-band applications. The unit cell is of simple shape. The absorber is fabricated on a thin polyamide, which makes it flexible. The parameters of the designed absorber are optimized. The simulated results show that it has good absorption rate and polarization stability. The stability is exhibited over a wide range in both TE and TE modes of the incident waves. The measured results are on par with the simulated results. The measurement is carried out with the waveguide measurement method.

1. Introduction

Metamaterials are the artificial manmade periodic structures that are widely used in the design of antennae, frequency selective surfaces, and absorbers. The fact is that it has an unusual property that is not readily available in nature, i.e., negative consecutive parameters, antiparallel group, and phase velocities. In the year 2008 [1], a perfect electromagnetic metamaterial absorber is proposed and it paved the way for many researchers to focus on the design of EM-based metamaterial absorbers in the past two decades. There is a huge demand for the design of EM-based metamaterial absorbers with lighter compact and thinner configurations. A wide variety of structures has been introduced by the researchers by which the performance of the absorbers had been increased. Metamaterial absorbers that are insensitive to polarization are presented [2–4]. The multimode absorbers available are reported [5–7]. In [5], Xu et al. proposed an absorber with a complex shape, but the rate of absorption at the third frequency is very low. In [6], with complex and larger unit cell sizes, an absorber with triband frequency is presented. However, optimizing the performance of the band separately is difficult, even by changing its corresponding physical parameters. In [7], three I-shaped absorbers for THz frequency are reported and it was presented that the peak absorbance of more than 90% was noticed at the largest angle of incidence (60°). Metamaterial absorbers couple E and H fields separately. The absorbance was reported as above 88% at 11.5 GHz. The designers left a valuable suggestion of optimizing the design at the exact resonant frequency by choosing a highly consistent substrate with respect to its dielectric constant. A triband absorber is presented in [1], which uses two resonators. A triangular metamaterial absorber using plasma material is reported in [8]. The developed structure consists of three layers, namely, metal, dielectric, and solid-state plasma (SSP) layers (realized by GaAs), producing the polarization-independent absorption at the rate of absorption greater than 90% across 11.76 GHz–14.43 GHz spectrum. The designers also explored its tuneable performance by exciting the different solid-state plasma resonators.

In [9], the absorber with THz range is proposed and a hybrid metamaterial absorber (MA) with high performance with two absorption peaks, which were obtained by electrical and cavity modes of resonance, respectively, in [10]. The method to decrease the operating frequency of the unit cell of an MA (towards 1.35 GHz) was discussed in [11], which was aimed to make the absorber more suitable for practical applications as well as to reduce the sensitivity with respect to the curvature of the structure, leading 88% fractional bandwidth with good absorption for 0°–40° incidence angles. Another miniaturized MA was designed and proposed in [12], which operates in the UHF band (86–960 MHz) for UHF-RFID applications for enhancing the reliability of the RFID system. A THz range MA was demonstrated in [13] with a novel combinatorial approach provided with a nested structure composed of multiple metal-dielectric layers. In [14], a cross-shape unit cell with a flexible substrate is presented, and it was reported that the stretch of 25% was causing a resonant frequency shift of 0.5% for TM polarization. Wide-angle polarization-insensitive characteristics absorbers are presented in [15], and the structure uses a metallic background plane, four groups of pins to connect a metallic ring around which there are four groups of dipoles. Liquid crystal was used in the mesh voids to impart tunability for the F frequency band absorber in [16], in which the variation in the bias voltage causes the frequency tunability of 6.4% and proposed this design for developing the tuneable absorbers and sensors. The tuneable absorption characteristics (claimed to be the biggest in the range of 77.10%) were reported in [17] at 3 μm central wavelength, which was obtained by the reversible phase transition of VO_2 between metallic and dielectric states. Two square ring resonators were used of different sizes and fabricated on felt material to prepare a wearable metamaterial absorber in [18]. The deformation effect was also studied claiming that the design provides high absorptivity at 9.475 GHz targeting the indoor radar clear applications. An absorber in [19] is with an active configuration that can be electrically controllable in terms of polarization and frequency. The active nature was implemented by inserting PIN diodes between the circular ring and Jerusalem cross structures of the absorbers. In [20], with metallic incurved structure, an absorber is presented for the UHF-RFID and 4G applications and a relative bandwidth of 108% is reported, and a two-concentric-circular-split-ring-based absorber in the X-band range is presented in [21].

In [22], a split-ring-cross resonator (SRCR), metallic ring, and meander line are used to design the absorber. The designers identified that the lowering of operating frequency has decreased the electrical size of the unit cell through the inductance and capacitance generated by the metallic patterns. A quad-band ultrathin MMA was proposed in [23], which uses cross dipoles loaded with split-ring resonators forming the unit cell structure resonating at 3.68/8.58/10.17/14.93 GHz, respectively, showing a high absorption in both TE and TM polarizations. The design proposed in [24] reports the absorber with a two-dimensional metallic structure and operates in two modes, namely, localized surface plasmon (LSP) mode and dielectric loss mode, which contributes to multiband absorption characteristics. Even though a large number of absorbers are reported in the literature, they have a very complex rigid structure with fabrication complexity. Thus, there is a huge demand for the design of metamaterial absorbers with good performance such as multiband, flexible, compact, and low-cost fabrication.

In this paper, we propose a metamaterial [25–32] absorber that exhibits three different absorption peaks. A metamaterial-based ultrabroad band absorber is proposed at the THz range. The absorbers are based on the Ti/Ge/Si3N4/Ti. Two types of absorbers are proposed based on the different combinations and both achieved the ultrawideband response. In [33], a multilayered metamaterial with graphene is proposed for dual-band application. The operating frequency of the proposed absorber is 0.79–20.9 GHz and 25.1–40.0 GHz. The proposed absorber is the combination of the multiple graphene layers and the metamaterial absorber. In [34], the split-disk-based tunable absorber works at THz frequency application; in [35], broadband metamaterial absorber based on CMA is presented for S, C, X, and Ku bands; and in [36–38], metamaterial absorber, which is used for solar energy harvesting, is proposed. The proposed structure is having significant features such as the triple-band, polarization-insensitive, compactness, and simple shape that end in easy fabrication. The flexible nature of the proposed absorber makes it useful for the microbolometer, spectral imaging, and coating material. The absorber is proposed, where the absorptivity is more than 90% at the peak absorption frequencies [39–41].

2. Unit Cell Design

The geometry of the absorber unit cell is shown in Figure 1. The design consists of the patch, ground, and substrate, where its patch consists of a block line border, which is spaced by a 0.5 mm, at the center of the unit cell, cross having a rhombic-shaped patch element with a spacing value of 0.5 mm and four rectangular strips with triangular pointing structures looking outwards from the center towards corners of the unit cell.

The proposed geometrical structure of the unit cell is designed on the polyimide substrate with a thickness of 0.1 mm, which imparts compactness in terms of the overall volume of the absorber. The absorber's absorption is characterized by $A = 1\text{-R-T}$, where the background will be made up of the metals, which makes the transmissivity zero. The parameters of the unit cell are optimized properly such that the incident wave is properly coupled. The simulation of the proposed absorbers is carried out using Ansoft HFSS with PBC as its boundary condition.

3. Results and Discussion

3.1. Absorptivity Characteristics. It undergoes master-slave periodic boundary conditions. Mathematically, it can be obtained by the equation $A(\omega) = 1 - R(\omega) - T(\omega)$, which can be rewritten as follows:

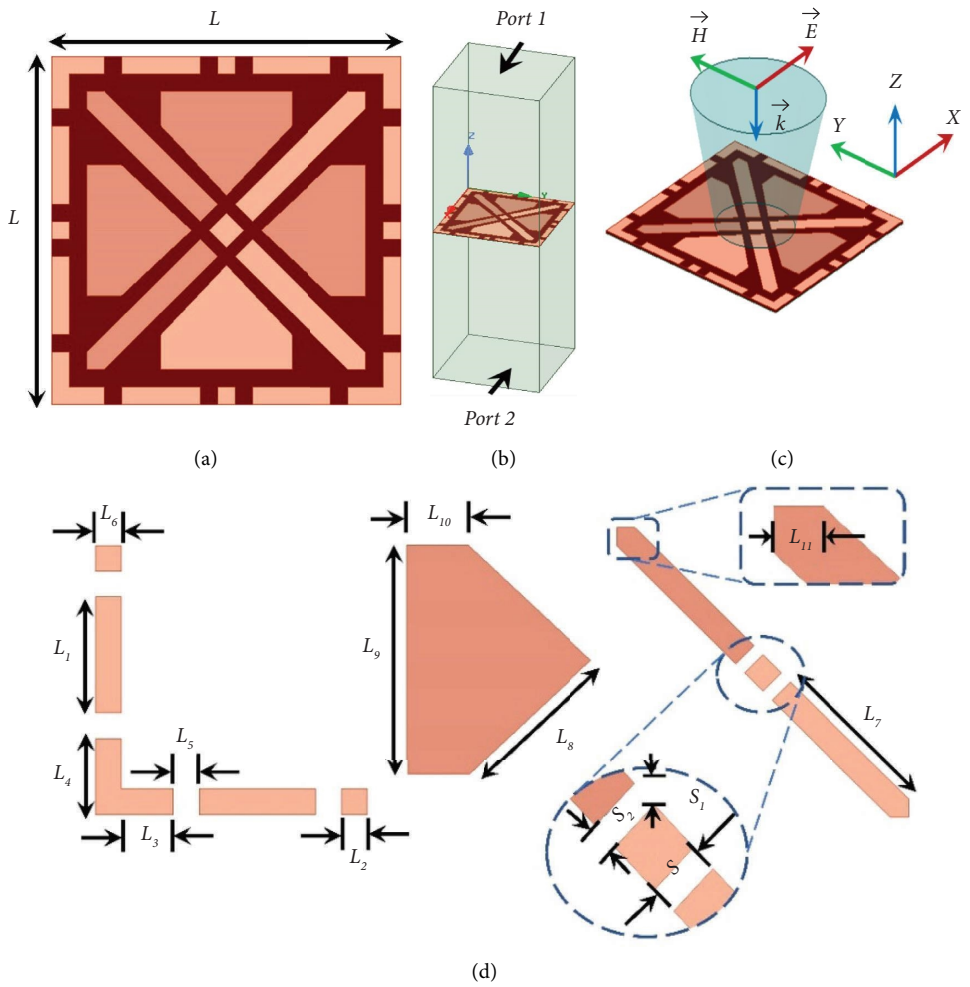

Figure 1: Structure of the proposed unit cell: (a) unit cell geometry; (b) Floquet port simulation; (c) schematic representation of incident field; (d) geometrical parameters: $L = 10$, $L_1 = 2.25$, $L_2 = 0.5$, $L_3 = 1$, $L_4 = 1.5$, $L_5 = 0.5$, $L_6 = 0.5$, $L_7 = 4.6$, $L_8 = 2.75$, $L_9 = 3.75$, $L_{10} = 1$, $L_{11} = 0.5$, $S = 0.7$, $S_1 = 0.5$, $S_2 = 0.35$, and $T = 0.1$ (all dimensions are in mm).

To analyze the absorptivity of the absorber unit cell,

$$A = \left(A - \left|S_{11}(\omega)\right|^2 - \left|S_{21}\omega\right|^2\right), \tag{1}$$

where as $R(\omega) = |S_{11}(\omega)|^2$ and $T(\omega) = |S_{21}(\omega)|^2$ are the reflected power and transmitted power, respectively. But the ground plane is covered fully, so the ground plane acts as an obstacle for the incident wave and gives a zero transmission as a result. So, the equation can be written as

$$A = \left(1 - \left|S_{11}(\omega)\right|^2\right). \tag{2}$$

Figure 2 shows the simulated absorptivity values of the absorber, the absorber has two absorptivity peaks where the absorption is above 90%, and it is created at 11.4 GHz and 19.2 GHz frequencies where the absorption values at those peaks are 0.9753 and 0.9652, respectively. The absorption peaks are created one in the X-band and other in the K-band. There are many variations in the absorptivity by varying the incident angles.

Figure 3 represents the absorptivity values of the absorber by varying the incident angles for TE polarization,

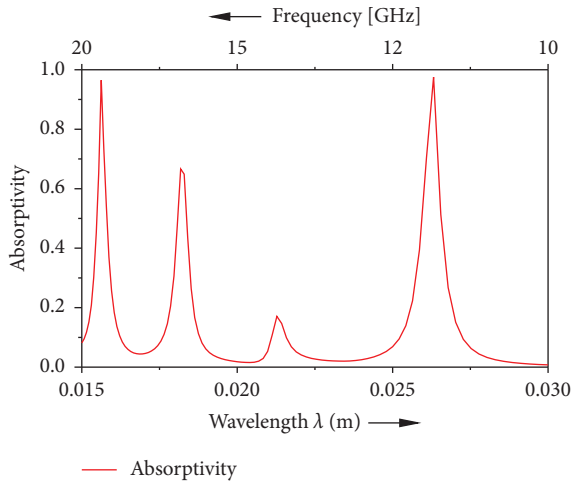

Figure 2: Absorptive characteristics.

where the incident angle ranges from 10 degrees to 90 degrees by a varying factor of 10 degrees. The absorption values are higher at incident angle phi 90 degrees, where the

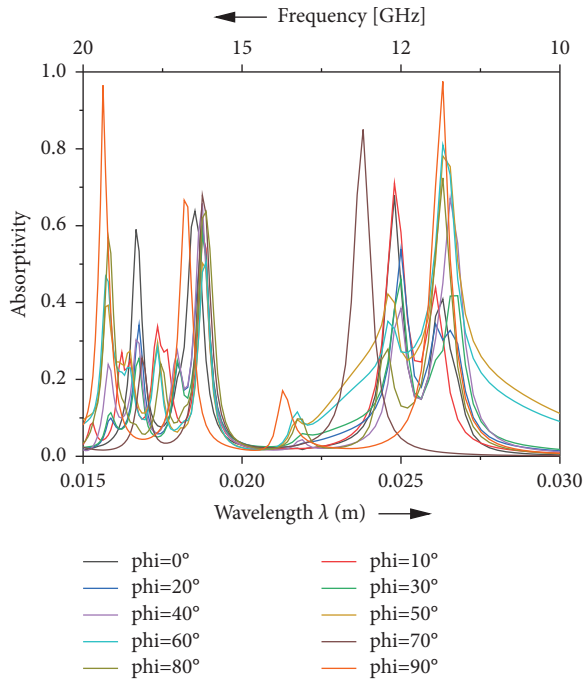

Figure 3: Absorptivity simulated for multiple angles of phi.

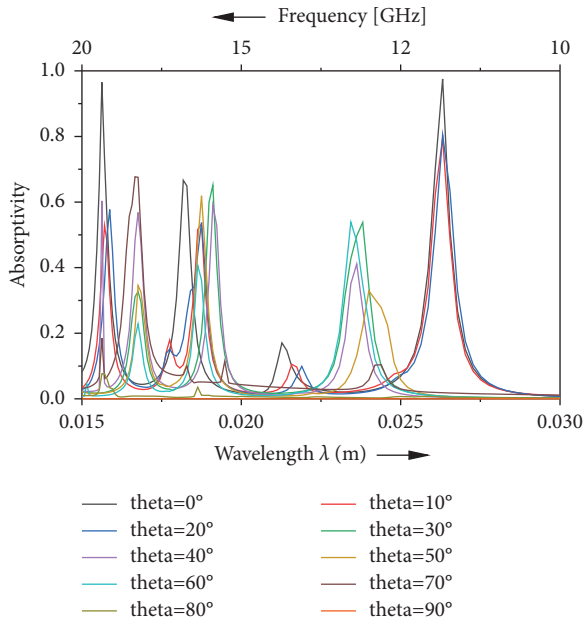

Figure 4: Absorptive simulated for multiple angles of theta.

values are greater than 0.9 at two different frequencies and at different frequency bands. Figure 4 represents the absorption values of the absorber achieved by varying the incident angles for TM polarization, which is same as TE polarization, but the absorption peaks are achieved at theta 0 degrees.

Conduction current (on the top and bottom conductors) and displacement current are created when the top and bottom layers' dominant current densities are antiparallel to one another (in between the top and bottom layer conductors through dielectric). At each of the peak absorption frequencies, a current loop is created by the conduction and displacement currents. This circulating current loop, which is centered on the incident magnetic field, causes magnetic excitation. The incident electric field at the top metallic surface causes electric excitation. Consequently, simultaneous electric and magnetic excitations take place.

3.2. Return Loss Characteristics. The return loss graphs are used to estimate the working of the structure, where the absorber achieved two resonance peaks one in x-band and the other in k-band where the return losses at those peaks are greater than −10 dB. The return losses with respect to the theta and phi are also simulated to know the relation between the graphs achieved and the achieved bands, where the theta0 and phi90 achieved the same values, as the absorption is achieved based on the values of the return loss; if the return loss is achieved for a particular structure, we can assume that the achieved working band in the return loss is also the same band for absorptivity is shown in Figure 5.

The reflection coefficient values are also achieved by varying the incident angles of TE polarization and TM polarization, where the results are good at theta0 and phi90, the peaks are achieved with respect to both the absorptivity and return loss where the simulated results TE and TM polarization are shown in Figures 6 and 7, respectively.

At oblique incidences, there is a slight difference between TE and TM. For TE polarization, the electric field is parallel to the top of the absorber, so most of the energy losses will be concentrated on the top layer. So, the absorptivity is more similar to the normal incidence. But in the case of TM polarization, the absorptivity is insensitive only if the dielectric loss is very high. At a low dielectric loss, the absorptivity loss is reduced with the increase in incident angle. This is due to the reason part which is depleted by the top layer and remailing is consumed by the dielectric substrate.

3.3. Fabricated Model. Here, the unit cells arranged into a group to achieve the absorbing characteristics in a wide area are shown in Figure 8(a). The structure designed is a 5×5 cell structure sheet where the spacing between each cell is 0.5 mm; an array of cells formed is shown in Figure 8(b). The measurement setup is shown in Figure 8(c).

In Figure 8(d), the equivalent circuit of the proposed absorber is presented. The capacitance c1 to c8 correspond to the rectangular and triangular slots in the proposed structure. The inductance L1 corresponds to the conductor ring between the slots, and the capacitor c9 denotes the diamond-shaped slot at the center. The inductance L2 and L3 correspond to the conductor length. The capacitance C10 and C11 denote the horizontal coupling between the unit cells, while the capacitors c12 and c13 denote the vertical coupling between the metal ring and the ground plane.

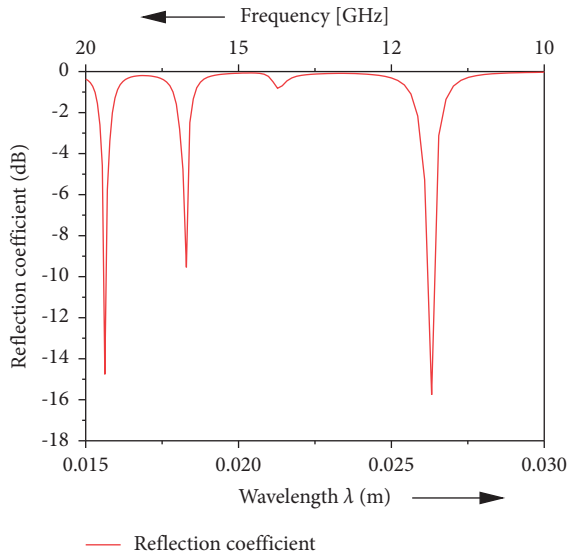

Figure 5: Reflection coefficient.

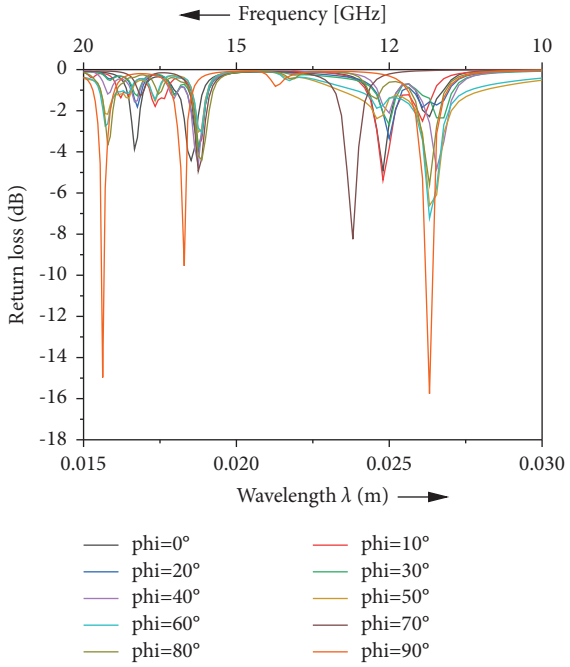

Figure 6: Return loss simulated for multiple angles of phi.

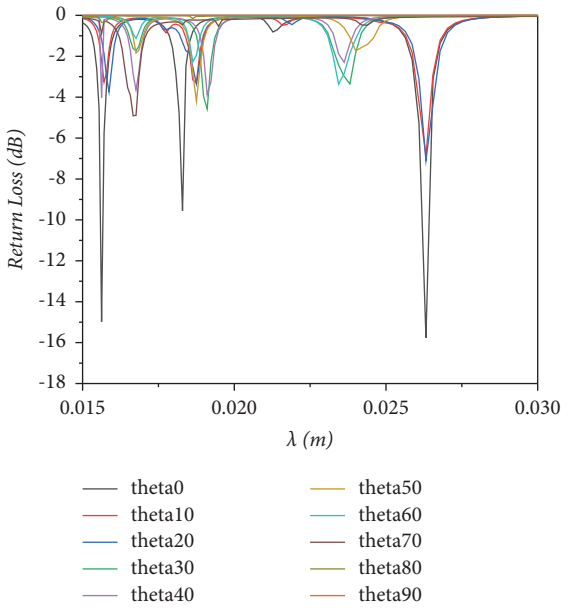

Figure 7: Return loss simulated for multiple angles of theta.

3.4. Measured Results. The proposed metamaterial absorber has achieved a good correlation between simulated and measured values of absorptivity, where the graph represents the simulated and measured values of the absorber. The proposed metamaterial absorber has achieved good correlation as shown in Figure 9.

Further to understand the radiation mechanism of the proposed structure, the surface current distribution of the proposed structure is studied. The performance analysis of the proposed absorber is shown in Table 1. Figure 10 shows the surface current distribution of the proposed structure at various resonating bands. It is observed that the current is centered around the metal strips and on the gaps in the structure. From Figure 10, it is observed that the current is around the outer square ring at 11.4 GHz. The absorption peak at 17.1 GHz is due to the X-shaped slots in the center of the square plate since the maximum surface current is higher around it at 17.1 GHz. The absorption peak at 19.2 GHz is due to the triangular slot in the square plate. The surface current flows strongly around the discontinuities leading to a strong electric and magnetic field in the opposite direction. Hence, the proposed structure simulates an equivalent LC, and its resonance can be adjusted by controlling the parameters.

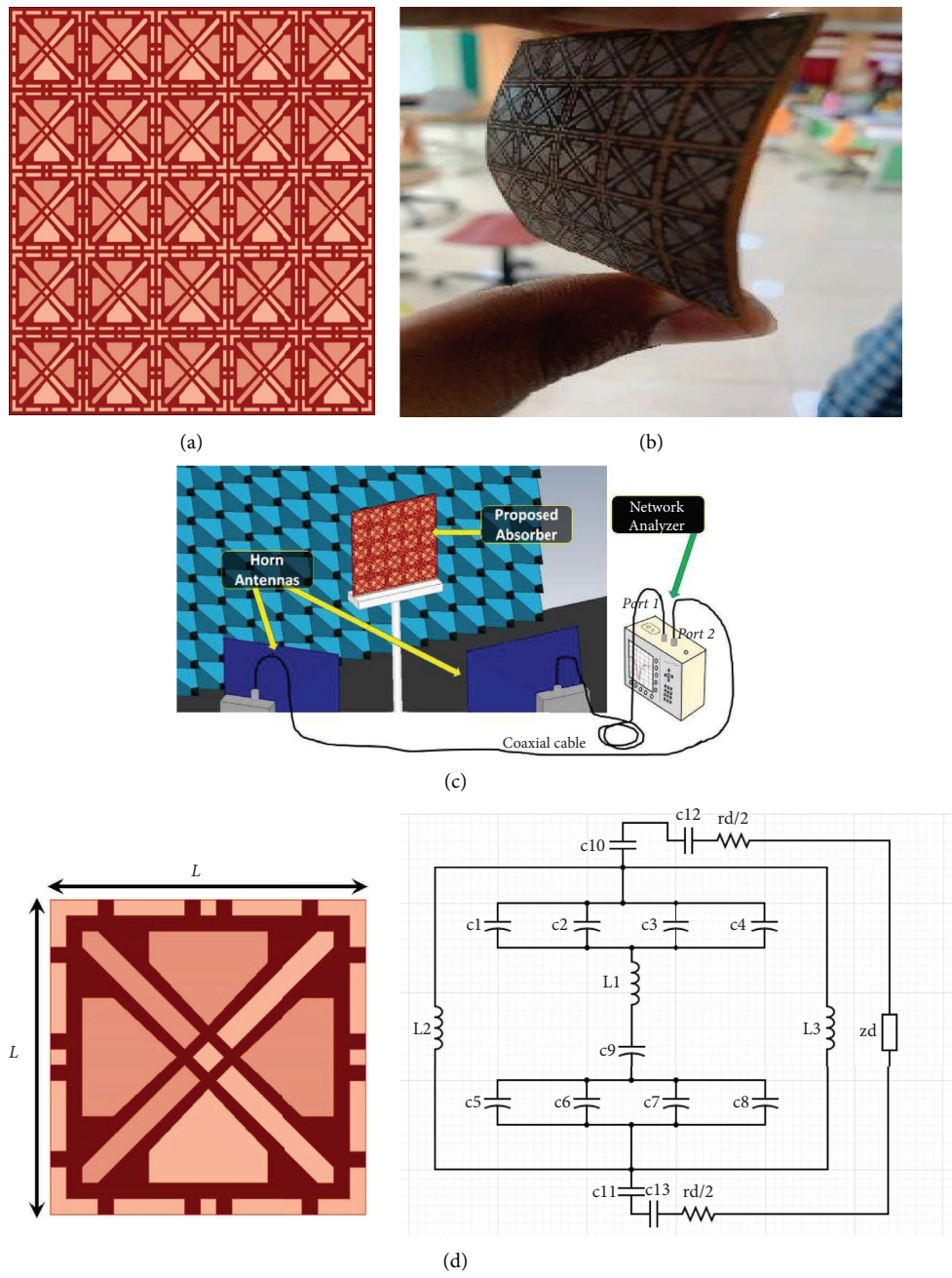

Figure 8: (a) Proposed absorber on thin substrate; (b) fabricated prototype; (c) measurement setup; (d) equivalent circuit.

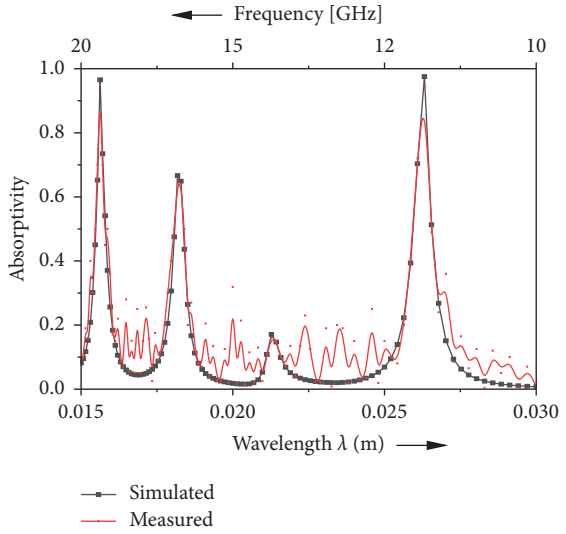

Figure 9: Measured vs simulated absorptivity.

Table 1: Performance analysis of the proposed absorber.

[Ref]	Configuration of the absorber	Operation center frequency/band (GHz)	Size of the unit cell (in mm)	No. of bands getting absorbed	Percentage of absorption (%)
[2]	Metamaterial resonators	11.5	$12 \times 4.2 \times 0.2$	1	>88
[4]	Metamaterial resonators	11.76–14.43	$72 \times 72 \times 3$	1	>90
[5]	Hybrid dielectric layer absorber	1.35–3.5	$20 \times 20 \times 1.6$	1	>90
[6]	Square loop loaded lumped resistor MMA	0.86–0.96	$20 \times 19.2 \times 1.6$	1	>90
[1]	Stretchable metamaterial absorber	11–11.4	$8 \times 8 \times 3$	1	>90
[8]	Ultrathin metamaterial absorber	3.25, 9.45, 10.9	$11 \times 11 \times 1.03$	3	>90
[11]	Wearable MMA	9, 9.85	$30 \times 30 \times 1$	2	>90
[12]	Active MMA	4.3, 5.9	$13.8 \times 13.8 \times 1$	2	>90
[13]	Ultrawide-band MMA	0.8–2.7	$20 \times 20 \times 1.6$	1	>90
Proposed	MMA	11.4, 17.1, and 19.2	$10 \times 10 \times 0.1$	2	>90

MMA = metamaterial-based absorber.

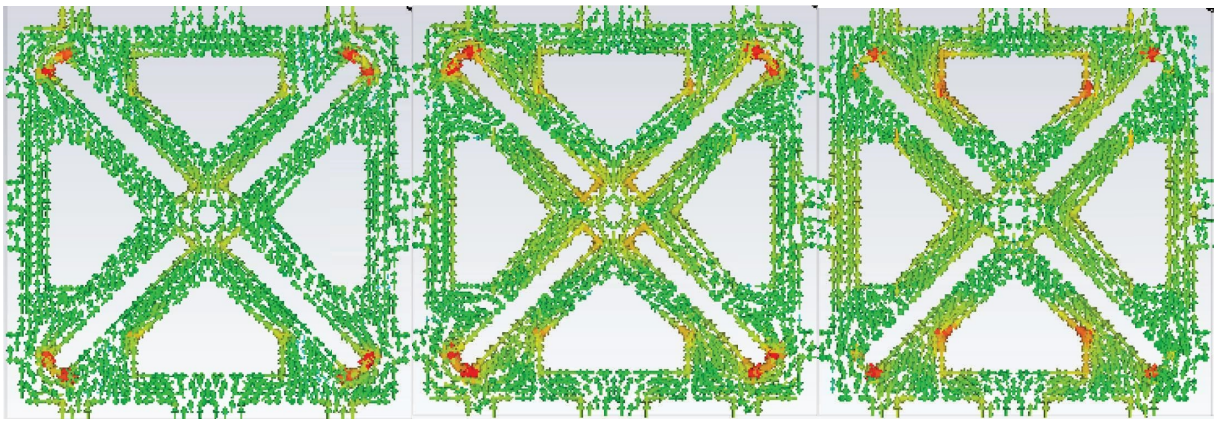

(a)11.4 GHz (b) 17.1 GHz (c)19.2 GHz

Figure 10: Surface current distribution at various resonating frequencies: (a) 11.4 GHz. (b) 17.1 GHz. (c) 19.2 GHz.

4. Conclusion

In this article, a new design is proposed to achieve a triband metamaterial-based ultrathin polarization-insensitive absorber. The absorber is flexible in nature. The bands are achieved by optimizing the parameters. The proposed absorbers exhibit absorption above 90% in the bands for the incident wave both in TE and TM. It also exhibits high polarization insensitivity over wide angles, making it suitable for the multimode metamaterial absorbers.

Data Availability

No data were used in this article.

Conflicts of Interest

The authors declare that they have no conflicts of interest.

Acknowledgments

The authors are thankful to the Center for Embedded Systems, Department of ECE, and QISCET.

References

[1] N. I. Landy, S. Sajuyigbe, J. J. Mock, D. R. Smith, and W. J. Padilla, "Perfect metamaterial absorber," *Physical Review Letters*, vol. 100, no. 20, Article ID 207402, 2008.

[2] O. Luukkonen, F. Costa, C. R. Simovski, A. Monorchio, and S. A. Tretyakov, "A thin electromagnetic absorber for wide incidence anglesand both polarizations," *IEEE Transactions on Antennas and Propagation*, vol. 57, no. 10, pp. 3119–3125, 2009.

[3] Q. Ye, Y. Liu, H. Lin, M. Li, and H. Yang, "Multi-band metamaterialabsorber made of multi-gap SRRs structure," *Applied Physics*, vol. 107, no. 1, pp. 155–160, 2012.

[4] J. Lee and S. Lim, "Bandwidth-enhanced and polarisation-insensitive metamaterial absorber using double resonance," *Electronics Letters*, vol. 47, no. 1, pp. 8-9, 2011.

[5] H. X. Xu, G. M. Wang, M. Q. Qi, J. G. Liang, J. Q. Gong, and Z. M. Xu, "Triple-band polarization-insensitive wide-angle ultra-miniature metamaterial transmission line absorber," *Physical Review B: Condensed Matter*, vol. 86, no. 20, Article ID 205104, 2012.

[6] S. Bhattacharyya, S. Ghosh, and K. Vaibhav Srivastava, "Triple band polar-ization-independent metamaterial absorber with bandwidth- enhance-ment at X-band," *Journal of Applied Physics*, vol. 114, no. 9, Article ID 094514, 2013.

[7] L. Huang, D. R. Chowdhury, S. Ramani et al., "Experimental demonstration of terahertz metamaterial absorbers with a broad and flat high absorption band," *Optics Letters*, vol. 37, no. 2, pp. 154–156, 2012.

[8] N. Mishra, D. K. Choudhary, R. Chowdhury, K. Kumari, and R. K. Chaudhary, "An investigation on compact ultra thin triple band polarization independent meta-material absorber for microwave frequency applications," *IEEE Access*, vol. 5, pp. 4370–4376, 2017.

[9] H. F. Zhang, H. Zhang, Y. Yao, J. Yang, J. X. Liu, and J. X. Liu, "A band enhanced plasma meta-material absorber based on triangular ring-shaped resonators," *IEEE Photonics Journal*, vol. 10, no. 4, pp. 1–10, 2018.

[10] J. Zhang, J. Tian, and L. Li, "A dual-band tunable metamaterial near-unity absorber composed of periodic cross and disk graphene arrays," *IEEE Photonics Journal*, vol. 10, no. 2, pp. 1–12, April 2018.

[11] M. Zhong, "A high performance and temperature sensitive absorber based on hybrid dielectric layers metamaterial," *Optics & Laser Technology*, vol. 112, no. 15, pp. 168–174, 2019.

[12] M. D. Banadaki, A. A. Heidari, and M. Nakhkash, "A metamaterial absorber with a new compact unit cell," *IEEE Antennas and Wireless Propagation Letters*, vol. 17, no. 2, pp. 205–208, 2018.

[13] W. Zuo, Y. Yang, X. He, D. Zhan, and Q. Zhang, "A miniaturized metamaterial absorber for ultrahigh-frequency RFID system," *IEEE Antennas and Wireless Propagation Letters*, vol. 16, pp. 329–332, 2017.

[14] W. Pan, X. Yu, J. Zhang, and W. Zeng, "A novel design of broadband terahertz metamaterial absorber based on nested circle rings," *IEEE Photonics Technology Letters*, vol. 28, no. 21, pp. 2335–2338, 2016.

[15] P. Zhou, L. Wang, G. Zhang et al., "A Stretchable metamaterial absorber with deformation compensation design at microwave frequencies," *IEEE Transactions on Antennas and Propagation*, vol. 67, no. 1, pp. 291–297, 2019.

[16] H. Zhai, C. Zhan, Z. Li, and C. Liang, "A triple-band ultrathin metamaterial absorber with wide-angle and polarization stability," *IEEE Antennas and Wireless Propagation Letters*, vol. 14, pp. 241–244, 2015.

[17] G. Deng, T. Xia, S. Jing, J. Yang, H. Lu, and Z. Yin, "A tunable metamaterial absorber based on liquid crystal intended for F frequency band," *IEEE Antennas and Wireless Propagation Letters*, vol. 16, pp. 2062–2065, 2017.

[18] Z. M. Liu, Y. Li, J. Zhang et al., "A tunable metamaterial absorber based on VO_2/W multilayer structure," *IEEE Photonics Technology Letters*, vol. 29, no. 22, pp. 1967–1970, 2017.

[19] J. Tak and J. Choi, "A wearable metamaterial microwave absorber," *IEEE Antennas and Wireless Propagation Letters*, vol. 16, pp. 784–787, 2017.

[20] X. Zeng, L. Zhang, G. Wan, and M. Gao, "Active metamaterial absorber with controllable polarisation and frequency," *Electronics Letters*, vol. 53, no. 16, pp. 1085-1086, 2017.

[21] W. Zuo, Y. Yang, X. He, C. Mao, and T. Liu, "An ultra-wideband miniaturized metamaterial absorber in the ultra-high-frequency range," *IEEE Antennas and Wireless Propagation Letters*, vol. 16, pp. 928–931, 2017.

[22] S. Ghosh, S. Bhattacharyya, D. Chaurasiya, and K. V. Srivastava, "An ultrawideband ultrathin metamaterial absorber based on circular split rings," *IEEE Antennas and Wireless Propagation Letters*, vol. 14, pp. 1172–1175, 2015.

[23] M. Yoo, H. K. Kim, and S. Lim, "Angular- and polarization-insensitive metamaterial absorber using subwavelength unit cell in multilayer technology," *IEEE Antennas and Wireless Propagation Letters*, vol. 15, pp. 414–417, 2016.

[24] A. Sarkhel and S. R. Bhadra Chaudhuri, "Compact quad-band polarization-insensitive ultrathin metamaterial absorber with wide angle stability," *IEEE Antennas and Wireless Propagation Letters*, vol. 16, pp. 3240–3244, 2017.

[25] S. Li, X. Ai, R. Wu, J. Chen, and T. Jiang, "Enhancement of multi-band absorption based on compound structure metamaterials," *Optics & Laser Technology*, vol. 115, pp. 239–245, 2019.

[26] P. J. C. Sam and N. Gunavathi, "A tri-band monopole antenna loaded with circular electric–inductive–capacitive metamaterial resonator for wireless application," *Applied Physics A*, vol. 126, no. 10, 2020.

[27] S. Prasad Jones Christydass and N. Gunavathi, "Octa-band metamaterial inspired multiband monopole antenna for wireless application," *Progress In Electromagnetics Research C*, vol. 113, pp. 97–110, 2021.

[28] S. Prasad Jones Christydass and N. Gunavathi, "Dual-band complementary split- ring resonator engraved rectangular monopole for GSM and WLAN/WiMAX/5G sub-6 GHz band (new radio band)," *Progress In Electromagnetics Research C*, vol. 113, pp. 251–263, 2021.

[29] A. Kavitha, S. Prasad Jones Christydass, J. Silamboli, K. Premkumar, and A. NazarAli, "Metamaterial inspired triple band antenna for wireless communication," *International Journal of Scientific & Technology Research*, vol. 9, no. 3, 2020.

[30] N. Ramya, M. Sujatha, T. Jayasankar, and P. Jones Christydass, "Metamaterial inspired circular antenna with DGS for tetra band application," *International Journal of Control and Automation*, vol. 13, no. 2, pp. 877–882, 2020.

[31] S. Prasad Jones Christydass and N. Gunavathi, "Design of CSRR loaded multiband slotted rectangular patch antenna," in *Proceedings of the 6th Biennial Applied Electro Magnetics Conference (AEMC -2017) by Maharashtra Institute of Technology*, pp. 19–22, Aurangabad, India, December 2017.

[32] S. Prasad Jones Christydass and N. Gunavathi, "Co-Directional CSRR inspired printed antenna for locomotive short range radar," in *Proceedings of the 2017 International Conference on Inventive Computing and Informatics (ICICI)*, Coimbatore, India, November 2017.

[33] S. Kannadhasan and R. Nagarajan, "Development of an H-shaped antenna with FR4 for 1-10GHz wireless communications," *Textile Research Journal*, vol. 91, no. 15-16, 2021.

[34] C. Zhang, S. Yin, C. Long, B. W. Dong, D. He, and Q. Cheng, "Hybrid metamaterial absorber for ultra-low and dual-broadband absorption," *Optics Express*, vol. 29, no. 9, Article ID 14078, 2021.

[35] Y. Zhang, P. Lin, and Y.-S. Lin, "Tunable split-disk metamaterial absorber for sensing application," *Nanomaterials*, vol. 11, no. 3, 2021.

[36] Y. Wu, H. Lin, J. Xiong et al., "A broadband metamaterial absorber design using characteristic modes analysis," *Journal of Applied Physics*, vol. 129, no. 13, Article ID 134902, 2021.

[37] S. Kannadhasan and R. Nagarajan, "Performance improvement of H-shaped antenna with zener diode for textile applications," *Journal of the Textile Institute*, vol. 113, 2022.

[38] Y. Qiu, P. Zhang, Q. Li, Y. Zhang, and W. Li, "A perfect selective metamaterial absorber for high-temperature solar energy harvesting," *Solar Energy*, vol. 230, pp. 1165–1174, 2021.

[39] H. Li, L. H. Yuan, B. Zhou, X. P. Shen, Q. Cheng, and T. J. Cui, "Ultrathin multiband gigahertz metamaterial absorbers," *Journal of Applied Physics*, vol. 110, no. 1, Article ID 014909, 2011.

[40] Q. Y. Wen, H. W. Zhang, Y. S. Xie, Q. H. Yang, and Y. L. Liu, "Dualband terahertz metamaterial absorber: design, fabrication, and characterization," *Applied Physics Letters*, vol. 95, no. 24, Article ID 241111, 2009.

[41] Y. Zhou, Z. Qin, Z. Liang et al., "Ultra-broadband metamaterial absorbers from long to very long infrared regime," *Light: Science & Applications*, vol. 10, no. 1, 2021.